

# Brightness of point application of fluorescent quinine tracer for surface waters

*Avaliação da luminescência do traçador fluorescente quinino: aplicação localizada em águas de superfície*

João Luís Mendes Pedroso de Lima<sup>1,2\*</sup> , Soheil Zehsaz<sup>1,2</sup> , Jean Leite Tavares<sup>3</sup> ,  
Maria Isabel Pedroso de Lima<sup>1,2</sup> 

## ABSTRACT

Fluorescent tracers have been widely used in hydrology. Recently, quinine started to be used as a fluorescent tracer for estimating the velocity of surface sheet flows over various soil surface conditions and environments. In the present work, the visibility of the fluorescent tracer (quinine) was assessed for various applications' forms of the tracer (liquid, ice cube with quinine and soaked sponge). The brightness intensity of all tracer forms was estimated for different hydraulic conditions (hydrostatic, linear, and rotational flows) and for clear water, and water with medium and high suspended sediment loads. Results show that, when used as a flow velocity tracer, liquid quinine solution has to be applied carefully into the water and should better be used on sheet flows, shallow overland flows or shallow still waters. Its visibility in deep and muddy flows is insufficient for surface velocity estimations. The sponge soaked with quinine solution, which partially floats, is better visible in clear waters or low-medium suspended sediment loads, regardless of the water depth. However, for high turbulence and rotational flows, the soaked sponge sinks and is no longer visible. The ice cubes showed better visibility in all tested flow water depths and suspended sediment loads, although, in very shallow depths (of millimetres), ice cubes cannot be used because they might not follow adequately the fluid motion, which also applies to the sponge.

**Keywords:** hydrologic tracers; flow visualization; flow velocities; free surface water flows.

## RESUMO

Em hidrologia, têm sido amplamente utilizados traçadores fluorescentes para o estudo de escoamentos. Recentemente, começou a ser utilizado quinino como um traçador fluorescente, para estimar a velocidade de escoamentos superficiais em lâmina de água para várias condições da superfície do solo e ambientais. Neste trabalho, a visibilidade do traçador fluorescente (quinino) foi avaliada para diversas formas de aplicação do traçador (líquido, cubo de gelo e esponja embebida). A luminescência das três formas de aplicação do traçador foi estimada para todas as condições hidráulicas testadas (condição hidrostática e escoamentos linear e rotacional) e para água límpida e com média e elevadas cargas sólidas suspensas. Concluiu-se que a solução líquida de quinino, inserida com cuidado na superfície da água, quando usada como traçador da velocidade de escoamento, deve ser utilizada preferencialmente em escoamentos superficiais em lâmina de água ou em águas paradas, pouco profundas. A sua visibilidade em escoamentos superficiais profundos e com elevadas cargas sólidas suspensas é insuficiente para estimar velocidades de escoamento. Por sua vez, a esponja embebida em quinino, que flutua parcialmente, apresenta o seu melhor desempenho em águas límpidas ou com baixa-média carga sólida suspensa, independentemente da profundidade da água. No entanto, para escoamentos fortemente turbulentos e rotacionais, a esponja submerge e o traçador deixa de ser visível. Os cubos de gelo com quinino apresentam melhor visibilidade em todas as profundidades de água testadas e cargas de sedimentos em suspensão, embora, em profundidades de água/escoamento muito pequenas (de alguns milímetros), os cubos de gelo não sejam recomendáveis por poderem não acompanhar adequadamente o movimento do fluido, o que também se aplica à esponja.

**Palavras-chave:** traçadores hidrológicos; visualização do escoamento; velocidade de escoamento; escoamentos com superfície livre.

<sup>1</sup>Universidade de Coimbra, Faculdade de Ciências e Tecnologia, Departamento de Engenharia Civil - Coimbra, Portugal.

<sup>2</sup>Marine and Environmental Sciences Centre, Aquatic Research Network - Coimbra, Portugal.

<sup>3</sup>Instituto Federal de Educação, Ciência e Tecnologia do Rio Grande do Norte - Natal (RN), Brazil.

\*Corresponding author: plima@dec.uc.pt

**Conflicts of interest:** the authors declare no conflicts of interest.

**Funding:** The research presented here was partly funded through the Portuguese Fundação para a Ciência e a Tecnologia (FCT), involving projects UIDB/04292/2020 and UIDP/04292/2020 granted to the Marine and Environmental Research Centre (MARE), and project LA/P/0069/2020 granted to the Associate Laboratory Aquatic Research Network (ARNET), supported by national funds. The second author was granted a PhD fellowship from FCT (ref. 2020.07183.BD).

**Received:** 10/08/2022 - **Accepted:** 04/05/2023

## INTRODUCTION

The study of flow velocities is fundamental for a variety of hydrological and engineering applications. There is often the need to assess the velocity in situations where there are linear and rotational flows, which are common in, e.g., rivers, channels, and effluent treatment systems (VON SPERLING, 1997) or when there is a combination of different surface velocity vectors, a common situation in large reservoirs and also in the oceans (KOSHEL *et al.*, 2019). The most common velocity estimations are associated with surface flows in rivers and channels. In recent years, many studies have been presented regarding various applications of methods for estimating velocity distribution in the water column for different hydraulic conditions (NIKORA; NIKORA; O'DONOGHUE, 2013; KUMBHAKAR *et al.*, 2021; ZHANG *et al.*, 2023). Certain studies have aimed at forecasting velocity profiles in vegetated open channel flows (NIKORA; NIKORA; O'DONOGHUE, 2013), while others have investigated the whole velocity profile, encompassing both vegetation canopy and overlying flooded flow regions (KATUL; POGGI; RIDOLFI, 2011). Moreover, some studies have scrutinized the velocity distribution profiles on specific sections (STEPHAN; GUTKNECHT, 2002).

Hydraulic tracer studies assume that the chosen tracer is inert and thus should represent the water flow. Salt tracer solutions are common, but normally have a higher density than fresh water; therefore, they may lead to tracer settling at the bottom. This happens, for example, in wetlands (WANG; JAWITZ, 2006; SPEER *et al.*, 2009; WAHL *et al.*, 2010).

Flow visualisation using tracers is a useful tool in the study of fluid dynamics as it provides a quick qualitative and quantitative description of the flow field, both of steady and unsteady regimes (GRAHAM, 1984; SMITS; LIM, 2012). Also, it has the advantage to have reduced interference with the flow. Other frequently used techniques, such as invasive velocity probes, are only able to provide information at discrete points within the flow field (BOITEN, 2008).

Visualisation techniques might use different types of tracers (e.g., particles, fluorescent or coloured dye, and thermal tracers) added to the flow to signal the fluid motion, which can be defined using optical or thermographic techniques, such as LASER systems, high-speed cameras, and infrared devices.

Fluorescent tracers have been widely used in hydrology (BUZÁDY; EROSTYÁK; PAÁL, 2006; LEIBUNDGUT; MALOSZEWSKI; KÜLLS, 2009; ZHANG *et al.*, 2010; TAURO *et al.*, 2012; DE LIMA *et al.*, 2021; DI BELLA; KHATAMIFAR; LIN, 2022; ZEHSZAZ *et al.*, 2022). These tracers are common tools to identify connectivity between groundwater supply points (e.g., sinkholes and karst windows) and discharge points (e.g., springs and wells) (BUZÁDY; EROSTYÁK; PAÁL, 2006; LEIBUNDGUT; MALOSZEWSKI; KÜLLS, 2009), although they are also useful for studying surface flows (TAURO *et al.*, 2012; DE LIMA *et al.*, 2021; ZEHSZAZ *et al.*, 2022). Flow visualisation using a fluorescent dye is also an effective technique to qualitatively investigate flow patterns for various configurations, which usually involve low flow velocities and small laboratory scale geometries (DI BELLA; KHATAMIFAR; LIN, 2022).

Whereas common dyes, which are less expensive and normally safer to use, such as food colouring, are visible under naked eye (given that there is sufficient ambient light) when they are applied into the water, fluorescent dyes depend on ultraviolet (UV) or LASER light to help clearly expose the tracer from the fluid (i.e., the dye fluoresces/glows under those lights). This property allows one to use fluorescent dyes under specific ambient conditions, in particular, low ambient light conditions. Of the commonly used fluorescent dyes,

fluorescein has been used since the end of the 19<sup>th</sup> century due to being detectable in low concentrations, although it has very poor stability under sunlight (DOLE, 1906; SMART; LAIDLAW, 1977).

Recently, de Lima *et al.* (2021) presented a proof of concept for using quinine as a fluorescent tracer for estimating the velocity of surface sheet flows over various soil surface conditions and environments. This technique, where quinine is injected in liquid form into the flow, was compared with other similar tracer techniques that use dye and thermal tracers, also in liquid form. It was reported that the quinine fluorescent tracer offered flow velocity estimates that were comparable to the other tracers' estimates, and that the main advantages of using the quinine tracer were the high visibility of this tracer under ultraviolet A (UVA) light for low luminosity conditions, small environmental impact, and low-cost. Zehsaz *et al.* (2022) further explored the functionality of quinine as a tracer to estimate runoff velocities over mulched, vegetated, and paved surfaces. The results from that study showed that the quinine fluorescent tracer can be used in different rural and urban areas to estimate sheet flow velocities.

This study further explores the applicability and performance of the quinine tracer by systematically testing its brightness intensity for various hydraulic conditions: (i) suspended sediment loads (turbidity); (ii) velocities; and (iii) water depths, using laboratory reservoirs and flumes, under controlled conditions. Pixel classification techniques were used to evaluate the tracer movement in time-lapse imagery to capture the dynamics of the fluorescent tracers.

## MATERIALS AND METHODS

### Laboratory setups and materials

Different laboratory setups and conditions were used in this experimental work (Figure 1): (a) hydrostatic conditions in acrylic reservoirs (parallelogram of base  $0.40 \times 0.65 \text{ m}^2$  for low water depths and  $0.85 \times 0.85 \text{ m}^2$  for higher water depths); (b) linear (1D) uniform flow in a laboratory flume sloping surface (0.15 m wide and 4.00 m long); (c) rotational movement on an acrylic rotating cylindrical reservoir (diameter of 0.25 m). The main purpose of the experiments was to appraise the brightness of the quinine fluorescent tracer when applied into the water in different forms and for different water turbidity and hydraulic conditions. The experimental laboratory tests were conducted in the Laboratory of Hydraulics, Water Resources and Environment of the Department of Civil Engineering, of the Faculty of Science and Technology of the University of Coimbra (Portugal). The flume identified in Figure 1b has been used in other laboratory studies (FERREIRA *et al.*, 2006; ABRANTES *et al.*, 2018; ISIDORO *et al.*, 2021), at the University of Coimbra, Portugal.

Because the quinine fluorescent tracer is only visible in darker ambient light conditions under UVA light, an ambient light-shielded environment was provided for conducting the experiments. The quinine solution was obtained by mixing water with quinine powder at a concentration of  $80 \text{ mg}\cdot\text{L}^{-1}$  (for higher brightness, see Zehsaz *et al.*, 2022). The tracer was applied in the following forms into the flow: (1) liquid solution injected with a syringe; (2) quinine solution ice blocks (hereinafter called cubes) placed at the water surface; and (3) sponge soaked with quinine solution also placed at the water surface. The liquid tracer volume was 10 mL (commonly used volume injected with a syringe, for similar hydraulic conditions and class of experiments) and the size of the ice and sponge was approximately  $0.040 \times 0.035 \times 0.010 \text{ m}^3$  in all experiments. The tracers were added carefully into and on the water surface to have a minimum disturbance

of the hydraulic conditions. Figure 2 shows the different materials and forms of the quinine tracer applications in the present set of experiments.

To generate a suspension of fine materials in the water, a non-organic soil was used. This soil (used in, e.g., Oliveira, Correia and Cajada, 2018) has a high content of clay/silt particles (64%), shows low plasticity (dry unit weight:  $W = 9.9 \text{ kN}\cdot\text{m}^{-3}$ ; plasticity index:  $PI = 2\%$ ; liquid limit:  $wL = 44.0\%$ ; plastic limit:  $wP = 42.0\%$ ) and is classified as a low plasticity silty soil (ML), according to ASTM (1998). Sediment load suspensions of  $2 \text{ g}\cdot\text{L}^{-1}$  and  $5 \text{ g}\cdot\text{L}^{-1}$  were used during the experiments (for both hydrostatic and non-hydrostatic conditions), which were considered medium and high suspended loads, respectively, for the purpose of these experiments (in the high suspended load, visibility under water was very limited).

During the experiments, a camera with a  $12.80 \text{ mm} \times 9.60 \text{ mm}$  ISOCELL 2L2 (S5K2L2) CMOS sensor was used to capture images with a resolution of  $4290 \times 2800$  pixels, and  $1920 \times 1080$  pixels for the video frame. The camera was fixed in a position parallel to the water surface and at a height of 1.20 m from the water surface (Figure 1). These images were analysed to estimate the brightness of the quinine tracer, as explained next.

**Laboratory procedure**

The assessment of the brightness intensity of all quinine tracer forms (liquid, ice, and soaked sponge — Figure 2) was carried out for all hydraulic conditions (hydrostatic, linear/1D flow and rotational movement — Figure 1) and for clear water and water with medium and high suspended loads, for the purpose of comparison.

**Brightness estimation of the quinine tracer**

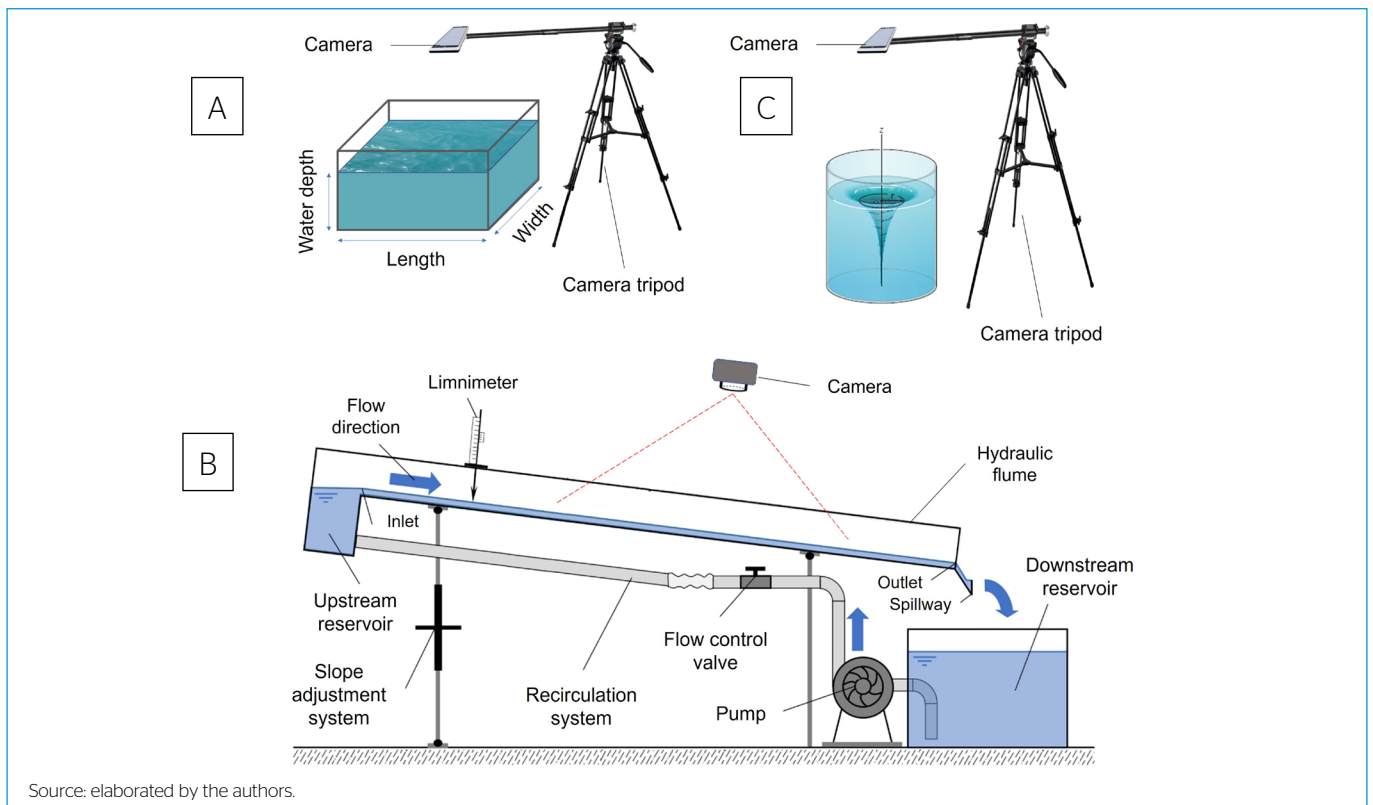
Every image consists of a set of pixels, which constitutes the raw building cells of the image. The pixels are defined in two categories: grayscale/single channel and colour. The pixels in an RGB colour space (colour image) have three colour channels: red, green, and blue. However, a grayscale image has just one channel and it usually uses an 8-bit representation for each pixel. A RGB image can be converted to a grayscale one by taking the weighted average of the red,

Syringe for the application of liquid tracer



Source: elaborated by the authors.  
 Note: The size of the ice and sponge was approximately  $0.040 \times 0.035 \times 0.010 \text{ m}^3$ .

**Figure 2** - Different materials and forms used for the quinine tracer application.



Source: elaborated by the authors.

**Figure 1** - Illustration of the laboratory setups for the three hydraulic conditions: a) hydrostatic; b) linear flow; c) rotational movement.

green, and blue components of each pixel in the image. The equation to convert RGB to grayscale is:

$$I = (0.2989 \times R) + (0.5870 \times G) + (0.1140 \times B) \quad (1)$$

Where R, G, and B are the red, green, and blue colour values of a pixel, respectively.

In this case, each pixel corresponds to a single scalar value ranging from 0 to 255. This number represents thus the brightness (lightness) intensity value of each pixel. Zero corresponds to “black” and 255 corresponds to “white” (STONE, 2003).

Analysis of the recorded image frames was conducted using the MATLAB image processing toolbox. All snapshots of the videos and images were converted to grayscale; therefore, the brightness intensity range for the fluorescent tracer varied from 0 to 255. The brightness intensity of the pixels that correspond to the tracer plume/stain in each image was extracted.

### Hydrostatic measurements

For evaluating the brightness of the quinine tracer, different water depths (0.01, 0.10, and 0.65 m) and suspended sediment loads (clear water and medium and high loads) scenarios were tested for hydrostatic conditions (Figure 1a). Three replicates of each of the experiments, which correspond to three independent photographs for each scenario, were undertaken.

### Linear flow measurements

A hydraulic flume was used for linear (1D) flow conditions (closed circuit — Figures 1b and 3). Experiments were performed for clear water and water with medium and high suspended sediment loads (2 and 5 g·L<sup>-1</sup>, respectively), like the no-flow (i.e., hydrostatic) experimental conditions.

For this hydraulic setup, the surface flow was fed at the upstream end of the flume through run-on from the feeder tank, which was controlled manually from the water pumping system using a valve until steady state flow was achieved. Once discharge became stable, the velocity measurements were undertaken with the installed video camera using the methodology described in de Lima *et al.* (2021). The movement of the tracer along the scanned area

(Figure 1b) was recorded in separated videos, for each tracer form and settings. The area scanned by the camera was established starting at 0.50 m downslope of the upstream end of the flume, with a dimension of 0.15 × 0.50 m<sup>2</sup> over the flume. Three replicates of the experiment were conducted for each flow discharge rate, which varied between 0.035 L·s<sup>-1</sup> and 1.530 L·s<sup>-1</sup>.

### Rotational flow measurements

The rotational flow measurements' setup is presented in Figures 1c and 4. The water movement was induced by rotating a cylindrical reservoir. The rotational velocities tested in this experiment were 5, 10, and 20 rpm, simulating vorticity in natural systems. Similarly to the other hydraulic conditions tested, all experiments were performed for clear water and water with medium and high suspended loads.

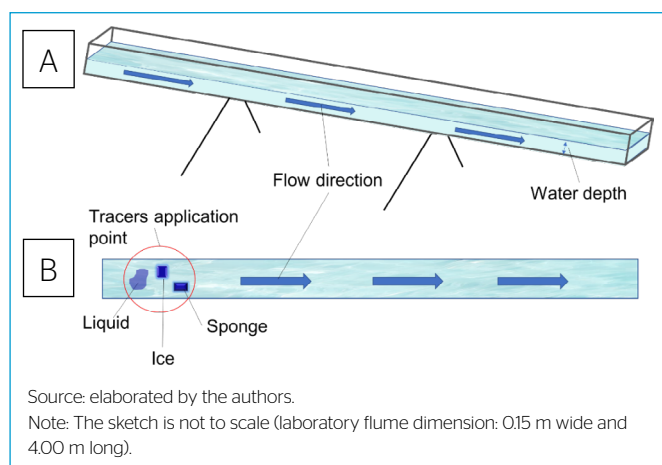
## RESULTS

### Still water conditions

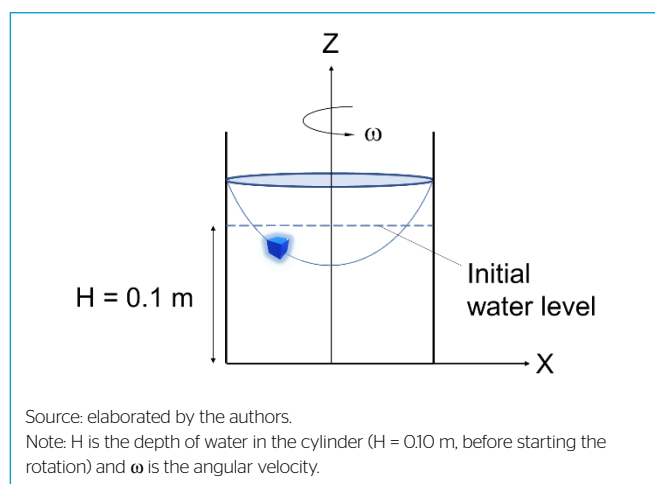
The difference between the visibility of the fluorescent (quinine) liquid solution, ice, and soaked sponge is illustrated in Figure 5 for the hydrostatic condition (i.e., horizontal water surface; no flow; no wind). The quinine liquid solution quantity used was the same, and the size of the tracers in ice and sponge forms were initially the same in all experiments; however, due to the melting of the ice, some snapshots might reveal different sizes for these two tracer forms.

Figure 5 shows that the visibility of the liquid form of application of the tracer diminishes as the height of the water column increases, since the liquid applied into the water sinks in the water column, moving away from the surface. Higher suspended sediment loads (i.e., muddy waters) further add difficulty to the visualization of the tracers. In this experiment, the tracer is only still visible from the surface for a water column depth of 0.65 m (the deepest water column tested) for clear water.

The brightness intensity (i.e., visibility) of the three forms of quinine tracer was plotted for the hydrostatic condition, and different water column depths and suspended sediment load (Figures 6 and 7). These figures show that the tracer liquid plume had the lowest brightness intensity in comparison to the ice



**Figure 3** - Illustration of the fluorescent tracer application for evaluating the brightness of quinine tracer in liquid, ice, and soaked sponge forms for linear uniform flow conditions: a) 3D view and b) top view.



**Figure 4** - Illustration of using quinine ice cube as a tracer for rotational flow movement in a rotating cylinder.

and soaked sponge form of application of the quinine tracer. The relatively low brightness intensity of the liquid quinine stain is due to dispersion and the fact the tracer sinks in the water column; many times, it attained values that were 50% less than the brightness of ice or sponge quinine tracers. In some cases, the tracer in liquid form could not even be detected.

For the experiments carried out for still water (hydrostatic) conditions, the brightness intensity found along transects defined for each of the plumes of the three tracer forms (liquid, ice, and sponge) was plotted in Figure 8. These transects contain the brightest pixel of each of the tracers' plumes; for the ice and sponge tracers, the transects are aligned with the longest dimension of their rectangular shape and, for the liquid tracer, imaginary circles were superimposed to the plumes and the transects contained the circles' centre and the brightest pixel in each image. Figure 8 shows that the liquid form of the tracer application had the biggest and the ice had the smallest plume area, visible from the top-view images of the water surface. The smallest size of the ice in comparison to the sponge at the time of measurements is due to the melting of the ice (the ice and the sponge were prepared for the experiments having the same size, see Figure 2). Nevertheless, although the ice plume had the smallest brightness areal coverage, it had a much higher average brightness intensity in comparison to the other two quinine tracer forms. In addition, although in the present experiments the average brightness of the sponge's plume is higher than that of the liquid tracer, the brightness is not homogeneous over the whole sponge surface due to the different pore sizes in the sponge structure. Figure 8 shows the mean values of three replicates of the experiments.

**Linear flows**

The brightness intensity of the three forms of quinine tracer applied into the water surface was explored for linear (1D) flow conditions, on the laboratory flume. For a clear water flow depth of 0.01 m, Figure 9 shows photographs of the applied tracers taken at time intervals  $\Delta t = 0.5$  s and Figure 10 shows, in each panel, two superimposed brightness intensity graphs corresponding to images captured with a time lapse of 1.0 s. It becomes clear that the ice had the highest brightness intensity in comparison to the other two forms of tracers and it

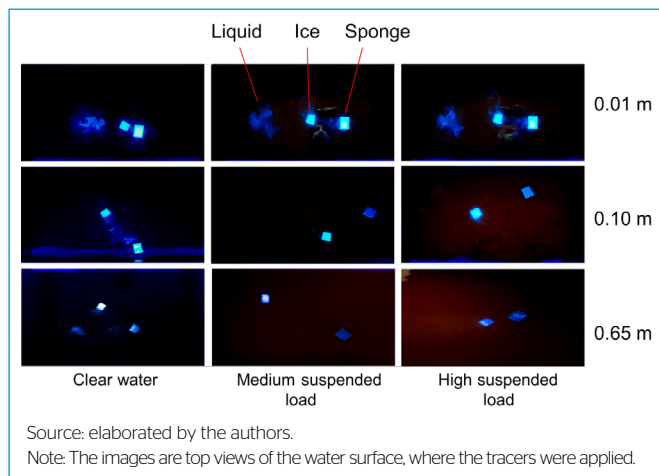


**Figure 5** - Illustrative comparison of the visibility of three types of application of quinine tracer (liquid, ice, and soaked sponge) in still waters, for water column depths of 0.01 m (top), 0.10 m (middle) and 0.65 m (bottom) and for clear water and two levels of suspended sediment loads.

remained approximately constant during the measurement time window, which is of a few seconds. For very shallow/sheet flows, small ice cubes should be used because, in these conditions, large ice particles can get stuck to the flume bed and eventually give wrong estimations of the flow velocity.

The same applies with respect to the size of the soaked sponges to be used. The quinine liquid solution had a good brightness intensity (i.e., good visibility) at the beginning of the experiment but that intensity tends to fade out over time, due to the dispersion of the tracer in the flow mass. After a  $\Delta t = 1.0$  s time lapse, the brightness level decreased significantly (i.e., 55%; Figure 10 — top). The sponge soaked with quinine solution maintained better its brightness level during each of the experiments' measurement time. At the beginning of each experiment,

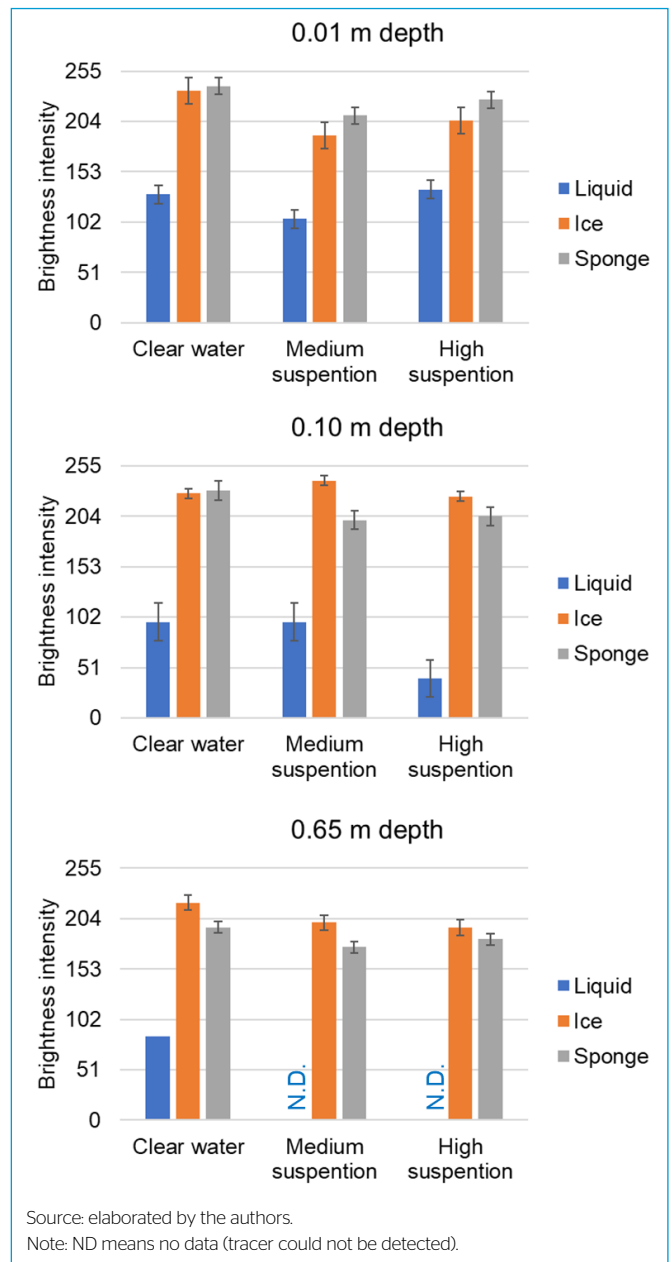


**Figure 6** - Brightness intensity of three fluorescent quinine tracer forms applied in still water conditions for different water column depths and levels of suspended fine materials loads (medium and high suspension loads correspond here to 2 and 5 g·L<sup>-1</sup>, respectively).

the soaked sponge brightness was lower than the brightness of the ice and liquid tracer forms, whereas 1 s after the tracers' application time the quinine solution's liquid plume manifested already a much smaller brightness than the sponge. The ice cubes have the tendency to melt over time, which might significantly reduce their visibility, depending on the original size of the ice cubes, the water temperature of the recipient, and the duration of the experimental tests.

In flowing waters with a high suspended sediment load, the quinine liquid solution plume could not be detected (Figure 11). Sponges soaked with quinine solution were observed to work well at the beginning of the tests but, after some time, as the sponge gets more soaked with the flowing water, it sinks in the water column and can no longer be detected. Also, for the type of sponge used, it was observed that, after using the same sponge for several times, it did not perform well and sunk rapidly. The sponges should be changed after one or two experimental trials.

Table 1 summarizes the data for surface flow velocity estimations using ice and sponge (average and standard deviation).

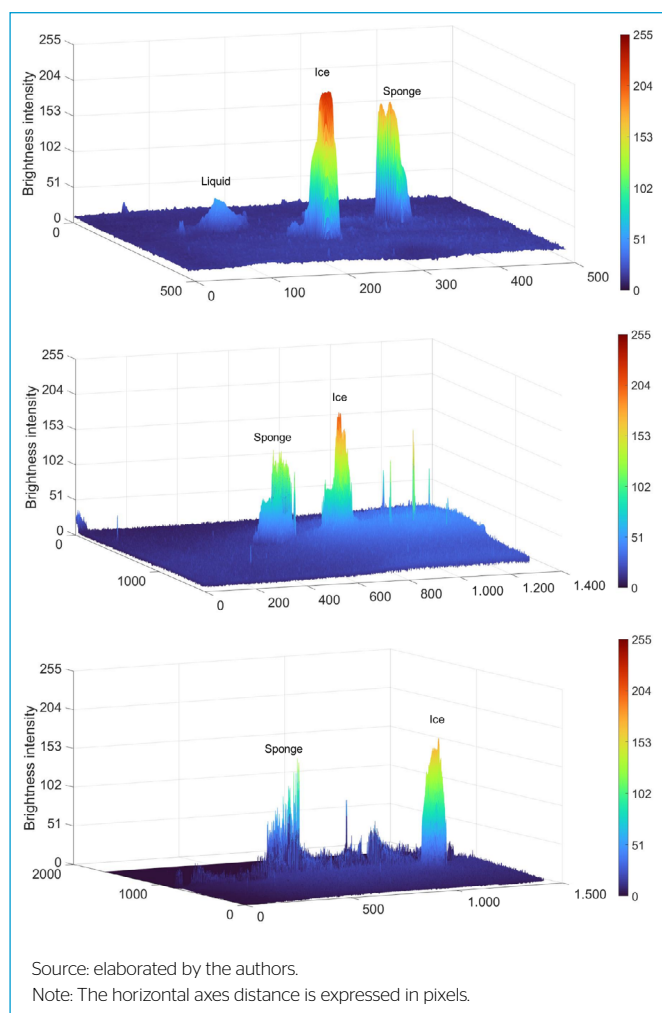


**Figure 7** - 3D illustration of the brightness intensity of all three forms of tracers at the same time and condition for the application of the tracers in still water conditions: clear water (top), medium suspension load (2 g·L<sup>-1</sup>; centre) and high suspension load (5 g·L<sup>-1</sup>; bottom), for the water depth of 0.65 m.

The analyses of results presented in Table 1 show that the applied tracer velocities, estimated by both techniques (ice and sponge), are similar under different suspended loads and similar discharges. The liquid form of the tracer had poor results in presence of sediments loads. It was not possible to visualise or track the leading edge of the liquid tracer in such turbid conditions. Therefore, no comparisons of velocity estimation were made between liquid and other tracer techniques.

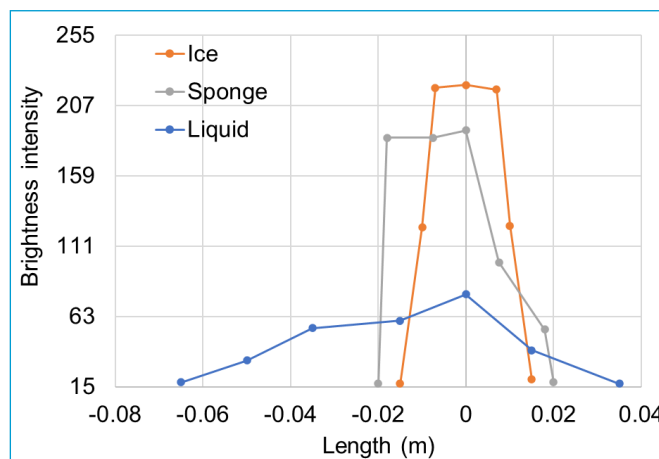
### Rotational flows

The comparison of the brightness intensity of the tracer in the form of ice cubes for clear water and medium and high suspended sediment loads is shown in Figure 12 for a rotational movement with a velocity of 20 rpm. Figure 12 shows that the suspended sediment load had no visible effect on the brightness of the quinine ice cubes, due to buoyancy. Several rotational velocities (5, 10, 20 rpm) were tested. The tracer in liquid and soaked sponge forms were also tested but these tracers did not deliver good visual results, since both were pulled down into the vortex. Only the ice cubes remained visible for all tested rotations.

### CONCLUSION

With respect to the brightness of point application of fluorescent quinine tracer into surface waters, the following conclusions could be drawn from this set of experiments:

- i. Liquid quinine solution, when applied as a flow velocity fluorescent tracer, should better be used on sheet flows and shallow overland flows and still water, in clear water environments. Its visibility in deep and muddy flows is many times insufficient for surface flow velocity estimations. Liquid quinine



Source: elaborated by the authors.  
Note: The zero of the x-axis contains the brightest pixel of each of the tracer plumes, with this axis supporting the representation of the variation of the tracer brightness intensity across transects identified for each of the plumes of the various tracer forms (liquid, ice, and sponge). Regardless of the actual positioning of the tracer plume in the image, for the ice blocks and sponges, the transects were defined along the longest dimension of their rectangular shape, containing the brightest pixel; for the liquid tracer, imaginary circles were superimposed to the plumes, and the transects contained the circles' centre and the brightest pixel in each image. The graph shows the mean values of three replicates.

**Figure 8** - Brightness intensity of the three tracer forms applied into still water, for a water column depth of 0.65 m.

tracer is not visible at the water surface in deeper water depths due to the sinking and diffusion of the tracer under the water surface. Only the use of large amounts of tracer could provide visible results; however, that would influence the hydraulic (or hydrostatic) conditions, which is not desirable.

- ii. The sponge soaked with quinine solution, which partially floats, exhibited better visibility in clear water and water with low-medium suspended sediment loads than the other forms of quinine tracer applications (liquid and ice), regardless of the water depth above a few millimetres. In very shallow flows (water depths of millimetres), soaked quinine sponges can no longer be used because they can get stuck or delayed in contact with the bed surface roughness elements. For high turbulent and rotational flows, the soaked sponge sinks and it is no longer visible (brightness due to fluorescence is no longer detected). It is expected that similar results are obtained for other sponge sizes, i.e., that the brightness of the quinine applied in this form (soaked sponge) supersedes the brightness of the other application forms (liquid and ice).
- iii. When compared with other forms of fluorescent quinine tracer applications, the ice cubes had overall better performance (i.e., higher brightness) in all tested flow water depths and suspended sediment loads, although, in shallow water depths, it is better to use smaller ice cubes because of the floating characteristic of the ice. Like the sponge, in very shallow water flow depths (of millimetres), ice cubes can no longer be used because they can get stuck or delayed in contact with the bed surface roughness elements.

Overall, the conclusion is that, of all three forms of fluorescent tracers used, the ice cubes have the best performance in terms of brightness (thus, visibility), for the investigated conditions. However, the quinine tracer's ability to follow the fluid motion was not analysed in this paper, which explored only the brightness intensity of the quinine fluorescent tracer. It is likely that rigid floating ice cubes with quinine may follow the fluid motion worse than the liquid quinine solution or, in some cases, worse than the flexible sponge.

**ACKNOWLEDGMENTS**

The research presented here was partly funded through the Portuguese Fundação para a Ciência e a Tecnologia (FCT), involving projects UIDB/04292/2020 and UIDP/04292/2020 granted to Marine and Environmental Research Centre (MARE), and project LA/P/0069/2020 granted to the Associate Laboratory

Aquatic Research Network (ARNET), supported by national funds. The second author was granted a PhD fellowship from FCT (ref. 2020.07183.BD).

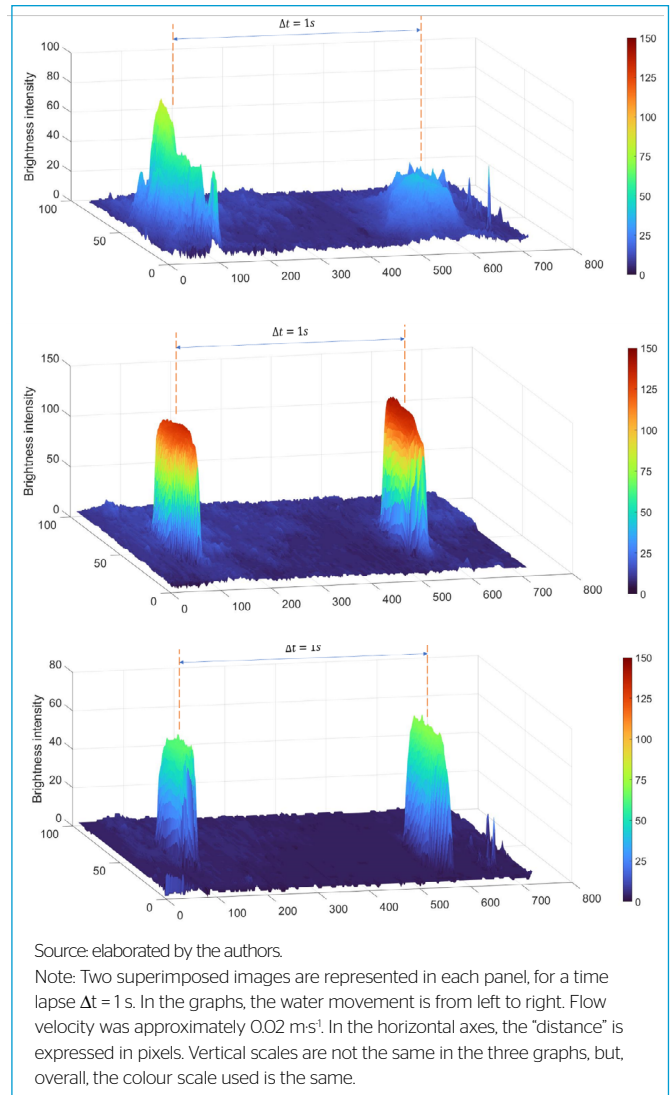


**Figure 10** - 3D illustration of the variation in brightness intensity of three tracer forms of liquid (top), ice cube (centre) and soaked sponge (bottom) applied in linear flow condition for a clear water depth of 0.01 m.

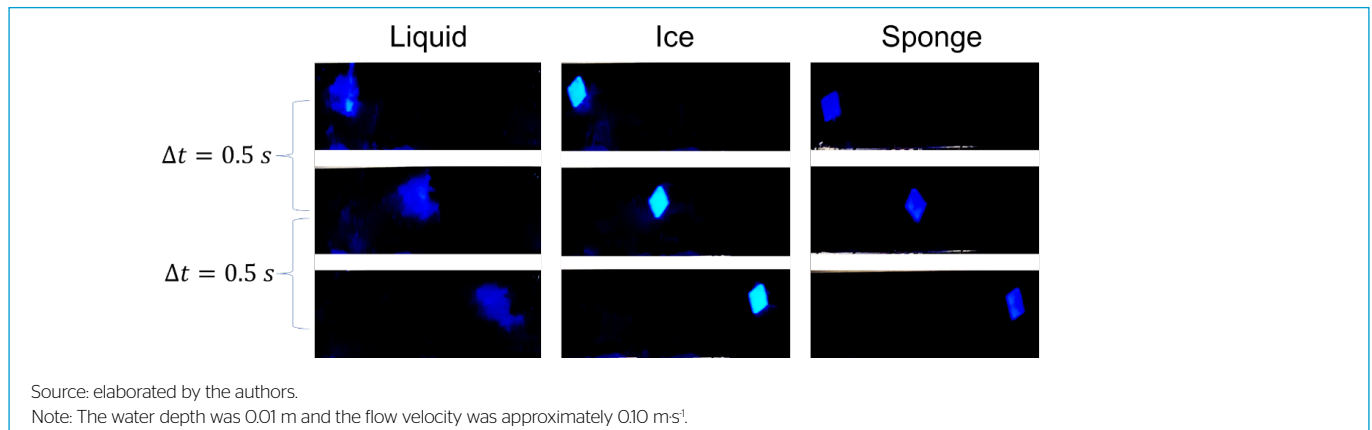


**Figure 9** - Comparison of the visibility of three forms of quinine tracer applied into clear water, for linear (1D) flow.

The experiments were conducted at the Laboratory of Hydraulics, Water Resources and Environment of the Department of Civil Engineering of the University of Coimbra (Portugal). The authors would also like to thank Professor P.J. da Venda Oliveira, of the Laboratory of Geotechnics of the Department of Civil Engineering (University of Coimbra), for providing the clay material used in the experiments conducted with muddy water.

### AUTHORS' CONTRIBUTIONS

de Lima, J.L.M.P.: Conceptualization, Funding acquisition, Methodology, Supervision, Writing – original draft, Writing – review & editing. Zehsaz, S.: Data curation, Investigation, Visualization, Writing – review & editing. Tavares, J.L.: Investigation. de Lima M.I.P.: Funding acquisition, Writing – review & editing.

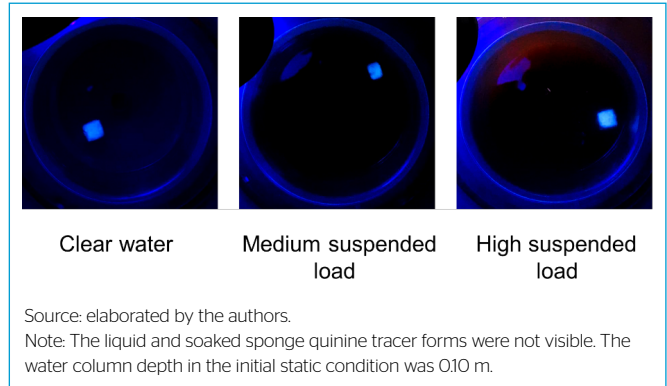


**Figure 12** – Comparison of the brightness intensity of quinine tracer ice cubes in a circular water movement with a velocity of 20 rpm, and different suspended sediment loads.

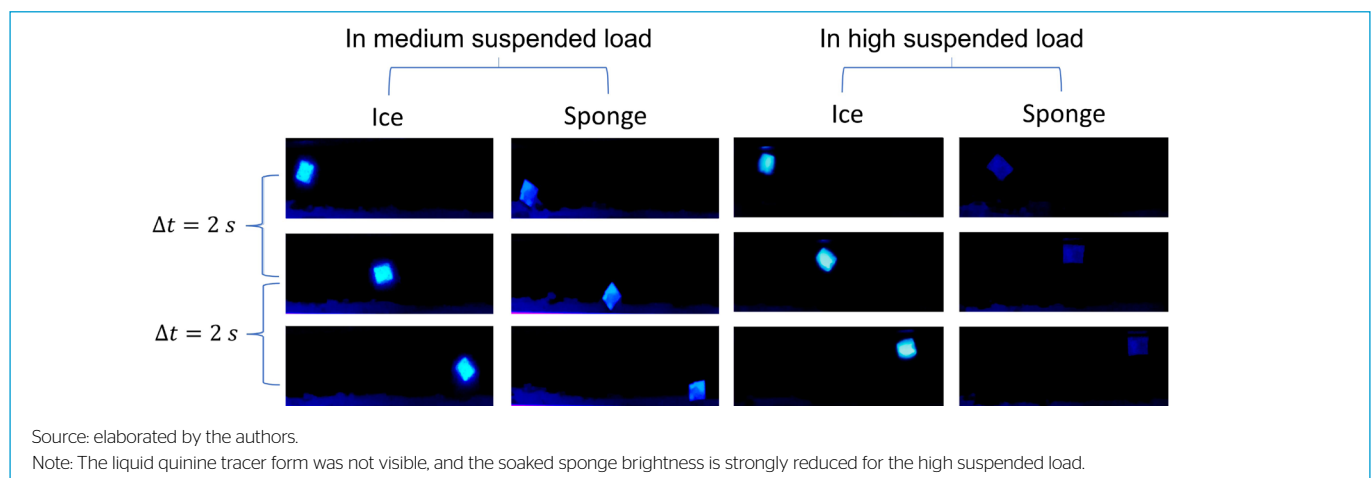


**Figure 11** – Comparison of the visibility of two forms of quinine tracer (ice and sponge) for medium and high sediment suspended loads (linear movement condition with a flow depth of 0.10 m).

**Table 1** – Surface flow test results for ice and sponge with linear flow conditions under different suspended loads, water depths and discharges.

| Discharge (L·s <sup>-1</sup> ) | Water depth (m) | Test number | Velocity U (m·s <sup>-1</sup> ) |        |                       |        |                     |        |
|--------------------------------|-----------------|-------------|---------------------------------|--------|-----------------------|--------|---------------------|--------|
|                                |                 |             | Clear water                     |        | Medium suspended load |        | High suspended load |        |
|                                |                 |             | Ice                             | Sponge | Ice                   | Sponge | Ice                 | Sponge |
| 153                            | 0.1             | 1           | 0.120                           | 0.110  | 0.120                 | 0.130  | 0.113               | 0.102  |
|                                |                 | 2           | 0.140                           | 0.115  | 0.110                 | 0.100  | 0.110               | 0.095  |
|                                |                 | 3           | 0.130                           | 0.116  | 0.100                 | 0.120  | 0.120               | 0.085  |
|                                |                 | 4           | 0.110                           | 0.104  | 0.120                 | 0.110  | 0.120               | 0.101  |
|                                |                 | Mean        | 0.125                           | 0.111  | 0.112                 | 0.115  | 0.115               | 0.095  |
|                                |                 | SD          | 0.011                           | 0.004  | 0.008                 | 0.011  | 0.004               | 0.006  |
| 153                            | 0.01            | 1           | 1.060                           | 1.110  | 1.070                 | 1.050  | 1.090               | 1.060  |
|                                |                 | 2           | 1.065                           | 1.115  | 1.090                 | 1.060  | 1.110               | 1.070  |
|                                |                 | 3           | 1.060                           | 1.105  | 1.100                 | 1.070  | 1.115               | 1.090  |
|                                |                 | 4           | 1.050                           | 1.090  | 1.100                 | 1.049  | 1.110               | 1.080  |
|                                |                 | Mean        | 1.058                           | 1.105  | 1.090                 | 1.057  | 1.106               | 1.075  |
|                                |                 | SD          | 0.005                           | 0.009  | 0.012                 | 0.0085 | 0.009               | 0.011  |
| 0.035                          | 0.01            | 1           | 0.022                           | 0.020  | 0.023                 | 0.022  | 0.024               | 0.023  |
|                                |                 | 2           | 0.024                           | 0.021  | 0.020                 | 0.025  | 0.025               | 0.022  |
|                                |                 | 3           | 0.025                           | 0.022  | 0.030                 | 0.025  | 0.023               | 0.024  |
|                                |                 | 4           | 0.025                           | 0.019  | 0.031                 | 0.021  | 0.023               | 0.024  |
|                                |                 | Mean        | 0.024                           | 0.020  | 0.025                 | 0.023  | 0.023               | 0.023  |
|                                |                 | SD          | 0.001                           | 0.000  | 0.004                 | 0.001  | 0.000               | 0.000  |

Source: elaborated by the authors.

Note: Mean values and standard deviations (SD) are for four replicates.

## REFERENCES

- ABRANTES, J.R.C.B.; MORUZZI, R.B.; SILVEIRA, A.; DE LIMA, J.L.M.P. Comparison of thermal, salt and dye tracing to estimate shallow flow velocities: Novel triple tracer approach. *Journal of Hydrology*, v. 557, p. 362-377, 2018. <https://doi.org/10.1016/j.jhydrol.2017.12.048>
- AMERICAN SOCIETY FOR TESTING AND MATERIALS (ASTM). *Standard Classification of Soils for Engineering Purposes (Unified Soil Classification System)*: D2487. West Conshohoken, PA: ASTM, 1998.
- BOITEN, W. *Hydrometry: A comprehensive introduction to the measurement of flow in open channels*. 3. ed. London: CRC Press, 2008. <https://doi.org/10.1201/9781003059288>
- BUZÁDY, A.; EROSTYÁK, J.; PAÁL, G. Determination of uranine tracer dye from underground water of Mecsek Hill, Hungary. *Journal of Biochemical and Biophysical Methods*, v. 69, n. 1-2, p. 207-214, 2006. <https://doi.org/10.1016/j.jbbm.2006.05.009>
- DE LIMA, J.L.M.P.; ZEHSZ, S.; DE LIMA, M.I.P.; ISIDORO, J.M.G.P.; JORGE, R.G.; MARTINS, R.G. Using Quinine as a Fluorescent Tracer to Estimate Overland Flow Velocities on Bare Soil: Proof of Concept under Controlled Laboratory Conditions. *Agronomy*, v. 11, n. 7, p. 1444, 2021. <https://doi.org/10.3390/agronomy11071444>
- DI BELLA, B.; KHATAMIFAR, M.; LIN, W. Experimental study of flow visualisation using fluorescent dye. *Flow Measurement and Instrumentation*, v. 87, p. 102231, 2022. <https://doi.org/10.1016/j.flowmeasinst.2022.102231>
- DOLE, R.B. Use of fluorescein in the study of underground waters. *Water Supply and Irrigation Paper*, n. 160, p. 73-85, 1906.
- FERREIRA, V.; GRAÇA, M.A.S.; DE LIMA, J.L.M.P.; GOMES, R. Role of physical fragmentation and invertebrate activity in the breakdown rate of leaves. *Archiv für Hydrobiologie*, Stuttgart, v. 165, n. 4, p. 493-513, 2006. <https://doi.org/10.1127/0003-9136/2006/0165-0493>
- GRAHAM, D.S. Fluorescent tracer mixing experiments in Glenmore Reservoir, Calgary. In: Annual Conference of the Canadian Society for Civil Engineering, 2, 1984. *Proceedings...* [s.l.]: Canadian Society for Civil Engineering, 1984, p. 989-1010.
- ISIDORO, J.M.G.P.; MARTINS, R.; CARVALHO, R.F.; DE LIMA, J.L.M.P. A high-frequency low-cost technique for measuring small-scale water level fluctuations using computer vision. *Measurement*, v. 180, 109477, 2021. <https://doi.org/10.1016/j.measurement.2021.109477>
- KATUL, G.G.; POGGI, D.; RIDOLFI, L. A flow resistance model for assessing the impact of vegetation on flood routing mechanics. *Water Resources Research*, v. 47, n. 8, W08533, 2011. <https://doi.org/10.1029/2010WR010278>
- KOSHEL, K.V.; STEPANOV, D.V.; RYZHOV, E.A.; BERLOFF, P.; KLYATSKIN, V.I. Clustering of floating tracers in weakly divergent velocity fields. *Physical Review E*, v. 100, n. 6, 2019. <https://doi.org/10.1103/PhysRevE.100.063108>
- KUMBHAKAR, M.; RAY, R.K.; CHAKRABORTY, S.K.; GHOSHAL, K.; SINGH, V.P. Mathematical modelling of streamwise velocity profile in open channels using Tsallis entropy. *Communications in Nonlinear Science and Numerical Simulation*, v. 94, 105581, 2021. <https://doi.org/10.1016/j.cnsns.2020.105581>
- LEIBUNDGUT, C.; MALOSZEWSKI, P.; KÜLLS, C. *Tracers in Hydrology*. Chichester: Wiley-Blackwell, John Wiley & Sons Ltd., 2009.
- NIKORA, N.; NIKORA, V.; O'DONOGHUE, T. Velocity profiles in vegetated open-channel flows: combined effects of multiple mechanisms. *Journal of Hydraulic Engineering*, v. 139, n. 10, p. 1021-1032, 2013. [https://doi.org/10.1061/\(ASCE\)HY.1943-7900.0000779](https://doi.org/10.1061/(ASCE)HY.1943-7900.0000779)
- OLIVEIRA, P.J.V.; CORREIA, A.A.S.; CAJADA, J.C.A. Effect of the type of soil on the cyclic behaviour of chemically stabilised soils unreinforced and reinforced with polypropylene fibres. *Soil Dynamics and Earthquake Engineering*, v. 115, p. 336-343, 2018. <https://doi.org/10.1016/j.soildyn.2018.09.005>
- SMART, P.L.; LAIDLAW, I.M.S. An evaluation of some fluorescent dyes for water tracing. *Water Resources Research*, v. 13, n. 1, p. 15-33, 1977. <https://doi.org/10.1029/WR013i001p00015>
- SMITS, A.J.; LIM, T.T. *Flow visualization: Techniques and examples*. London: Imperial College Press, 2012.
- SPEER, S.; CHAMPAGNE, P.; CROLLA, A.; KINSLEY, C. Hydraulic performance of a mature wetland treating milkhouse wastewater and agricultural runoff. *Water Science & Technology*, v. 59, p. 2455-2462, 2009. <https://doi.org/10.2166/wst.2009.332>
- STEPHAN, U.; GUTKNECHT, D. Hydraulic resistance of submerged flexible vegetation. *Journal of Hydrology*, v. 269, n. 1-2, p. 27-43, 2002. [https://doi.org/10.1016/S0022-1694\(02\)00192-0](https://doi.org/10.1016/S0022-1694(02)00192-0)
- STONE, M.C. *A Field Guide to Digital Color*. New York: A K Peters, 2003.
- TAURO, F.; GRIMALDI, S.; PETROSELLI, A.; RULLI, M.C.; PORFIRI, M. Fluorescent particle tracers in surface hydrology: a proof of concept in a semi-natural hillslope. *Hydrology and Earth System Sciences*, v. 16, n. 8, p. 2973-2983, 2012. <https://doi.org/10.5194/hess-16-2973-2012>
- VON SPERLING, M. *Lodos ativados: Princípios do tratamento biológico de águas residuárias*. 2. ed. Belo Horizonte: Editora da UFMG, 1997.
- WAHL, M.D.; BROWN, L.C.; SOBOYEJO, A.O.; MARTIN, J.; DONG, B. Quantifying the hydraulic performance of treatment wetlands using the moment index. *Ecological Engineering*, v. 36, n. 12, p. 1691-1699, 2010. <https://doi.org/10.1016/j.ecoleng.2010.07.014>
- WANG, H.; JAWITZ, J.W. Hydraulic analysis of cell-network treatment wetlands. *Journal of Hydrology*, v. 330, n. 3-4, p. 721-734, 2006. <https://doi.org/10.1016/j.jhydrol.2006.05.005>
- ZEHSZ, S.; DE LIMA, J.L.M.P.; DE LIMA, M.I.P.; ISIDORO, J.M.G.P.; MARTINS, R. Estimating sheet flow velocities using quinine as a fluorescent tracer: bare, mulched, vegetated and paved surfaces. *Agronomy*, v. 12, n. 11, 2687, 2022. <https://doi.org/10.3390/agronomy12112687>
- ZHANG, G.-H.; LUO, R.-T.; CAO, Y.; SHEN, R.-C.; ZHANG, X.C. Correction factor to dye-measured flow velocity under varying water and sediment discharges. *Journal of Hydrology*, v. 389, n. 1-2, p. 205-213, 2010. <https://doi.org/10.1016/j.jhydrol.2010.05.050>
- ZHANG, L.; GUAN, J.; ZHONG, D.; WANG, Y. Effect of sediment particles on the velocity profile of sediment-water mixtures in open-channel flow. *International Journal of Sediment Research*, v. 38, n. 3, p. 361-373, 2023. <https://doi.org/10.1016/j.ijsrc.2022.11.005>

